INTEGRATED PRESSURE AND VELOCITY MEASUREMENTS USING A SINGLE PRESSURE SENSOR ON THE CONE OF A WIND TURBINE

Konstantinos N. Antivachis and Anestis I. Kalfas
Department of Mechanical Engineering,
Aristotle University of Thessaloniki,
GR-54124 Thessaloniki, Greece

ABSTRACT

A new method of measuring 3D flow with a single pressure transducer mounted on the head of a wind turbines nose cone is presented in this paper. The principal of the proposed method is based on the five-hole probe calibration methodology. The novelty of the proposed method lays in the fact that a single rotating pressure tap on the wind turbines nose cone is used. Evidently, simplicity, functionality and applicability can be combined in industrial standard machines.

The pressure tap is directly connected to the transducer, which obtains four pressure measurements in four distinctive angular positions of the cone predefined by the calibration model. Thus the above measurements in the appropriate calibration coefficients obtain the flow field quantities such as yaw and pitch angle as well total and static pressure. Pressure taps have been made and calibrated on five distinctive diameters on the cone of a small-scale wind turbine in order to investigate the influence of the taps mounting on the calibration results. In addition, the effects of the wind turbine blades have been investigated. The proposed calibration coefficients results have been compared to results of an alternative model with an additional pressure tap located at the tip of the cone. While the precision of the model may improve, it may also increase the complexity of the measuring process. The coefficients different structural parts have been compared too, giving interesting conclusions about their impacts on the coefficients behaviour. The aforementioned process was implemented inside the low-pressure section of a wind tunnel. The results of this paper were acquired, using the above mentioned wind turbines nose cone, but they can easily be applied to any rotating single pressure probe.

The most spectacular outcome of this paper is the fact that, instead of using a probe with at least five-holes in order to obtain the full vector of a 3D flow, it is possible to achieve the same goal by using a single pressure probe, which has the ability to rotate. Therefore, the proposed method leads to a much smaller probe, which disturbs the flow a lot less, providing for a reduced measurement error. In addition, the calibration method becomes far less complicated. The cost reduction of the measuring process may be approximated by the difference between the manufacturing and running cost of a 5-hole probe and manufacturing and running cost of a single-hole pressure probe.

INTRODUCTION

In 3D flow measurements and especially in turbomachinery applications, the necessity of manufacturing probes as small as possible with the highest sensitivity and biggest angular range of operation have always been pursued. The most commonly used pressure probe until today has been the five-hole pressure probe, which has the least number of holes by which the full vector of any 3D flow can be defined using the classical calibration coefficients. Unfortunately, in most cases those probes are often larger than ideal, inducing errors that cannot be neglected in measuring results.

On the other hand, single sensor pressure probes can be typically made to be a half to a third of the size of multi-sensor probes [1] [2] [3]. Furthermore, when a single sensor is employed, the calibration is a lot simpler to define as well as more accurate as it does not involve multi sensor accuracy issues. In addition, the manufacturing complexity and the total construction costs are reduced. The results of this paper were acquired using a small-scale wind turbines nose cone in the low-pressure section of a wind tunnel. Nevertheless the same method can be implemented to any single pressure probe that has the ability to rotate.

Firstly, the behaviour of a dual pressure-sensor rotating probe is being analysed but the calibration method used is the classical five-hole probe method [4]. The basic difference lays in the fact that the measurements are being conducted in predefined angular positions, while the probe is rotating simulating a virtual five-hole probe. Secondly, new calibration coefficients are being presented requiring only one pressure sensor mounted on the nose cone. Those methods simplify a lot the measuring process but have also some disadvantages, which will be discussed in this paper. Thirdly, the impacts of the blades existence are examined too showing that they cannot be neglected since they induce large variations in the coefficients results.

EXPERIMENTAL SETUP

In order to investigate the ability of a wind turbines nose cone to estimate a flows vector by the way a pressure probe does, the nose cone of the small-scale wind turbine presented in Fig.1 was detached from its main construction and studied separately in laboratory conditions. In Fig.2 the cones drawing with its pressure tapings for several mounting diameters is presented.

Fig. 1: Small scale wind turbine

The tapings were made in various diameters, in order to investigate the pressure conditions on the cones surface. Another reason was to examine their mounting place effects on the calibration coefficients. Fig. 3 shows a significant variation on the tapings construction angle as the mounting diameter changes due to the geometry of the cone. Despite the fact that the measuring techniques presented in this paper, are applicable for single pressure taping arrangements, twelve pressure tapings have been made on each measuring diameter. An additional tapping had been made at the tip of the cone. This arrangement has been chosen in order to reduce the large amount of measurements required for the calibration procedure. In case there was only one pressure taping on each diameter the calibration procedure would last much longer, since except for the angular motion in the pitch and yaw angles the cone would also have to rotate. Using the currently proposed method, the calibration coefficients for a virtual 30^{O} roll angle step, can be obtained.

Two stepper motors were responsible for the motions of the cone in yaw and pitch angles and a digital pressure meter would register the pressure measurements. A fully automated program written in Labview programming language was used to conduct the process. The outcome of the measuring process was a set of 11,532 pressure measurements.

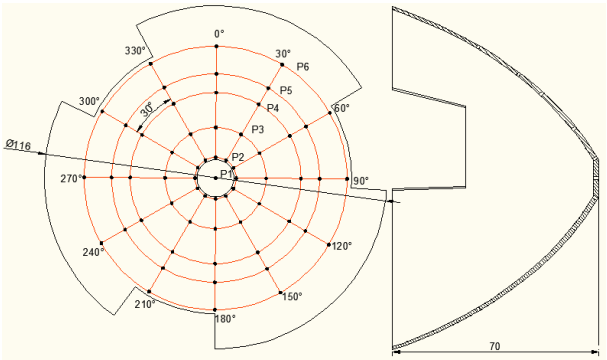

Fig. 2 : Nose cone dimensions and tapings

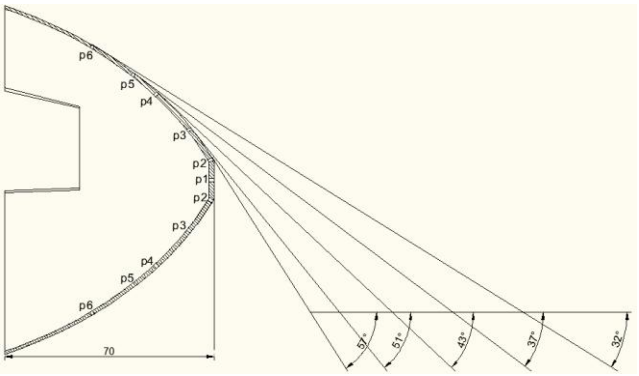

Fig. 3 : Probe construction angles and diameters

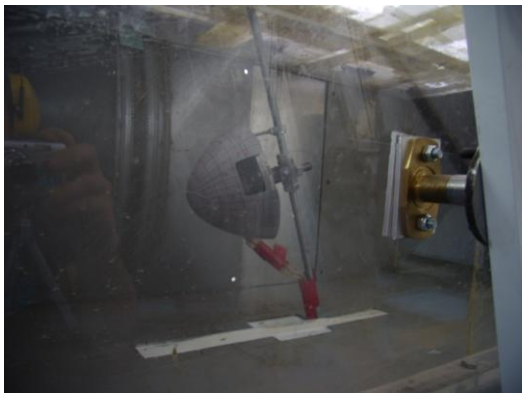

Fig. 4 : Nose cone inside the wind tunnel

In Fig. 4 the cone is depicted inside the wind tunnel during the measuring process. The range used for both yaw and pitch angles, is $\pm 30^{O}$ and the angular step used is 2^{O}. As a result, for each diameter of the cone, a file with 961 different combinations of yaw and pitch angles was produced. Each set of calibration data contains 12 pressure measurements intended for the reconstruction of a virtual single rotating pressure tap acquiring pressure data every 30^{O}, for each diameter. All of the measurements took place under the same free stream velocity of 10.5m/s in steady state conditions. The air density was $1.225 kg/m^3$ and the Reynolds number was stable at $8.2\ 10^4$.

CALIBRATION METHODOLOGY

TWO PRESSURE SENSOR ROTATING PROBE CALIBRATION METHOD

The distribution of the calibration coefficients are presented in the following figure 5.

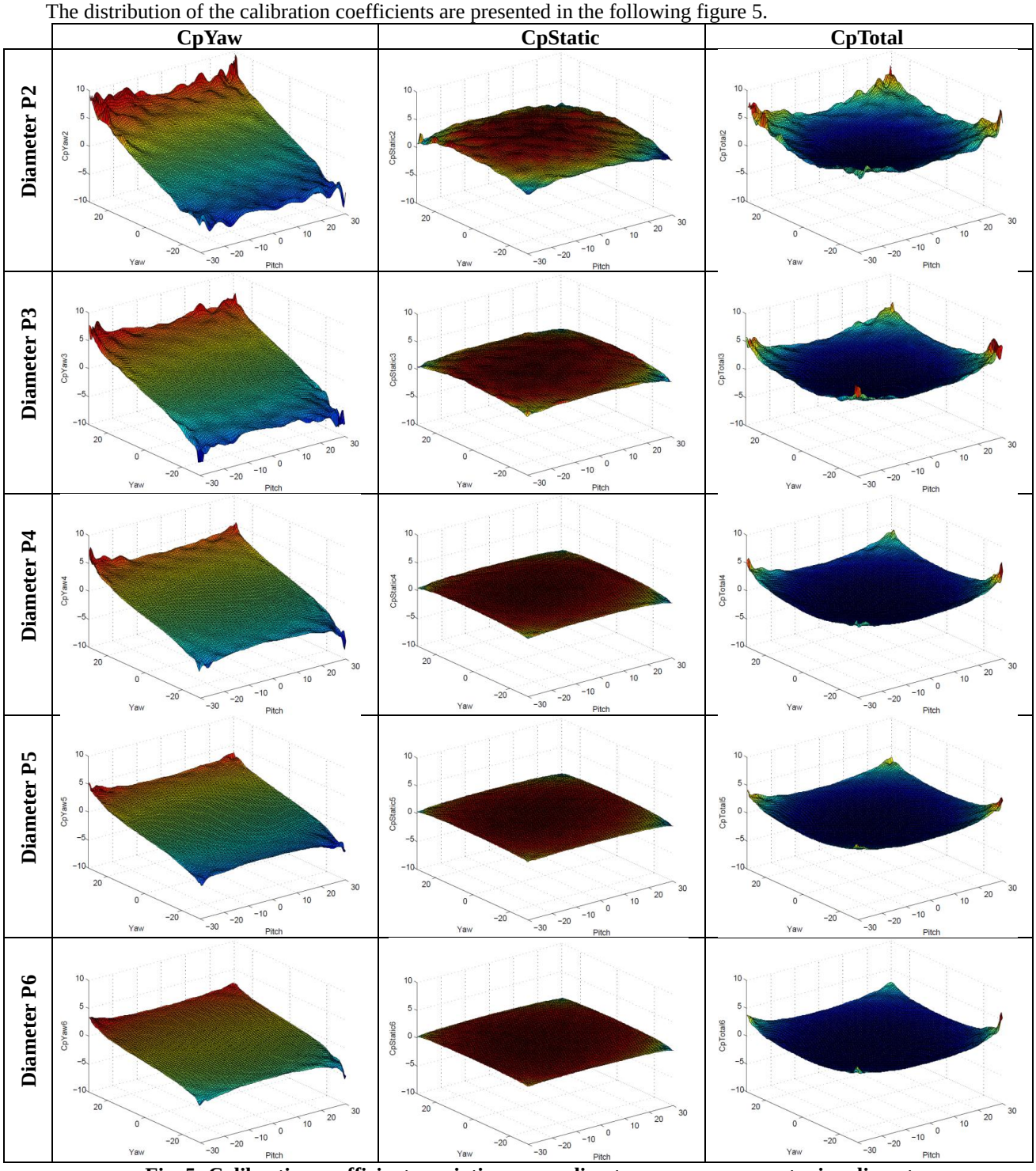

Fig. 5: Calibration coefficients variations according to pressure sensors taping diameter.

In this section, the coefficients of a two pressure sensor probe related to the yaw and pitch angles as well as the total and static pressure are presented.

$$Cp(i)pitch = \frac{P_i(180^0) - P_i(0^0)}{P_1 - (P_i(0^0) + P_i(90^0) + P_i(180^0) + P_i(270^0))/4} \quad (1)$$

$$Cp(i)yaw = \frac{P_i(270^0) - P_i(90^0)}{P_1 - (P_i(0^0) + P_i(90^0) + P_i(180^0) + P_i(270^0))/4} \quad (2)$$

$$Cp(i)static = \frac{P_1 - \mathrm{Pst}}{P_1 - (P_i(0^0) + P_i(90^0) + P_i(180^0) + P_i(270^0))/4} \quad (3)$$

$$Cp(i)total = \frac{Po - P_1}{P_1 - (P_i(0^0) + P_i(90^0) + P_i(180^0) + P_i(270^0))/4} \quad (4)$$

The "i" indicator stands for the pressure sensors taping diameter according to Fig. 2. The behaviour of each coefficient varies according to the diameter in which the pressure sensor is mounted. Those variations are presented in Fig. 5 for the coefficients of yaw angle, total and static pressure. The coefficient of pitch angle is not presented since it is almost identical with the yaw angles one. This happens because of the axial symmetry of the nose cone. The coefficients behaviour depends strongly on the pressure sensors taping diameter, which has a direct impact on the tapings construction angle.

In larger diameters the coefficients distinctiveness-sensitivity diminishes but the operational angular range of reliability raises. On the other hand in smaller diameters the coefficients sensitivity raises but the operational angular range of reliability diminishes. The diagrams of static and total pressure coefficients are smoother for larger diameters leading to much more trustworthy results. In addition their dependence from angular variations diminishes too. The behaviour of the pitch angle coefficient is approximately the same with yaw one but for some minor differences caused by construction errors in the symmetry of the cone. The above facts can be clearly observed, in the following four diagrams in which the reliable angular range and the gradient in both yaw and pitch angles of the yaw coefficient are presented.

In Fig. 6 the mean gradient of CpYaw in presented, which is the coefficient responsible for the yaw angles changes and its dependence from the sensors mounting diameter. It is clear that in smaller diameters which correspond to larger construction angles, such as p2 this gradient can be larger than four times the gradient in larger diameters such as the p6 one which corresponds to smaller construction angles.

In Fig. 7, the dependence of the CpYaw gradient from the sensors mounting diameter is presented. In this case, the focus is the pitch angle, which would be zero in the ideal case. In fact, there are construction errors, as well as measuring errors. This figure shows that there is some sensitivity-gradient, which is almost two orders of magnitude smaller than the gradient of the previous case. This is expected and, in any other case, it may be taken as a warning against systematic error, either with the measurements or the structural parts chosen for the specific coefficient.

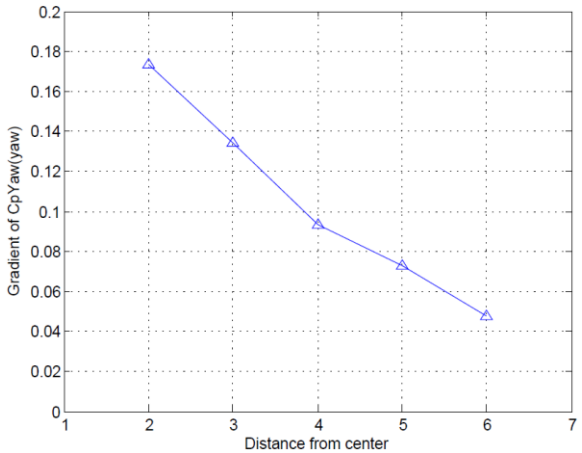

Fig. 6 : Gradient of CpYaw depending on the yaw angle for each diameter

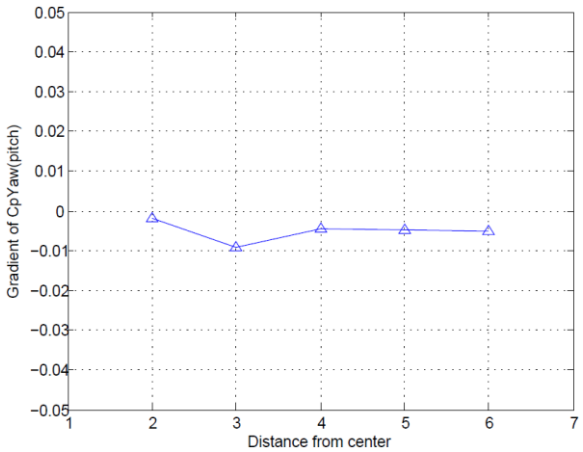

Fig. 7 : Gradient of CpYaw depending on the pitch angle for each diameter

In Fig. 8, the trustworthy range of the yaw coefficient is presented for each examined diameter. As trustworthy or beneficial range, in which a coefficient is operational is called the angular range in which this coefficient is considered capable to determine the angle of the flow with which it is charged for. This means that this range depends in its wholeness on the application in which the probe is going to be used in as well as the researcher's scope. So any method that tries to determine that range is a totally empirical method such as the one presented here.

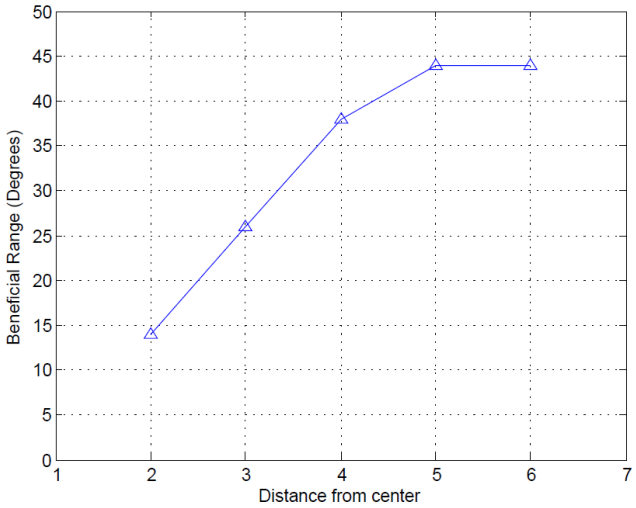

Fig. 8 : Trustworthy range for CpYaw for each diameter

More specifically, the proposed empirical method excludes from the trustworthy angular range the angles for which the yaw coefficient experiences intensive gradient variations for two consecutive pitch angles. The CpYaw coefficients values for the diameter p3 after the implementation of the aforementioned empirical method is presented in Fig. 9, which in comparison with the corresponding diagram of Fig. 5, provides further clarification in terms of the method as well as its application.

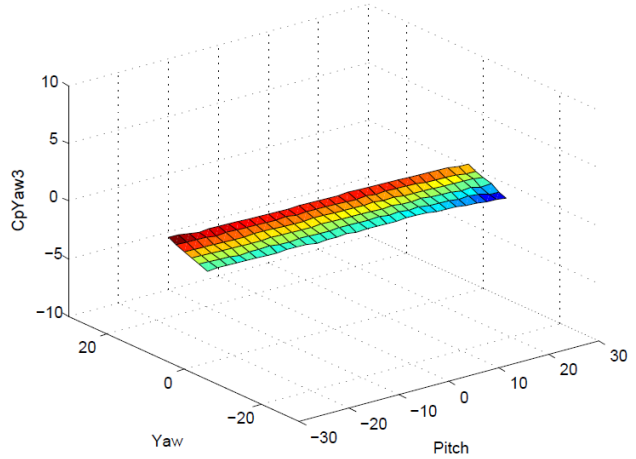

Fig. 9 : Trustworthy angular range for CpYaw coefficient

SINGLE PRESSURE SENSOR ROTATING PROBE CALIBRATION METHOD

In this section, four single pressure sensor probe calibration models are presented. The experimental part of the calibration process, is identical to the one used in the previous section for the two pressure sensor calibration probe. Each yaw and pitch angle combination (Fig.10) has a different impact on the nose cone's surface pressures. As a result, the characteristics of those unique contours for each angular combination could be captured by a single rotating pressure sensor mounted on the nose cones surface.

The reasons why the contours are not completely symmetric are structural and depend on the cone's geometry. As can be seen in Fig. 4 the cone is made out of casted plastic which obviously is not a very accurate treatment.

It has to be clear that the pressure results are differences between the atmospheric pressure and each pressure sensors measurement. This results to positive quantities since the experiment took place in the low pressure section of a wind tunnel. Hence the blue regions refer to higher pressures and the red ones to lower pressures. As mentioned before the pressure measurements were obtained for every 30^{O}. Hence for the construction of those diagrams a mathematical model of Fourier polynomial was used, which extrapolated those measurements.

Fig. 11 presents the same information with Fig. 10 for a specific pitch and yaw angle combination (30^{O}, 30^{O}), while it is also, presenting the pressure tapings diameters. Obviously, each taping is subjected to a different combination of pressures in a full rotation This can be clearly seen in Fig 12.

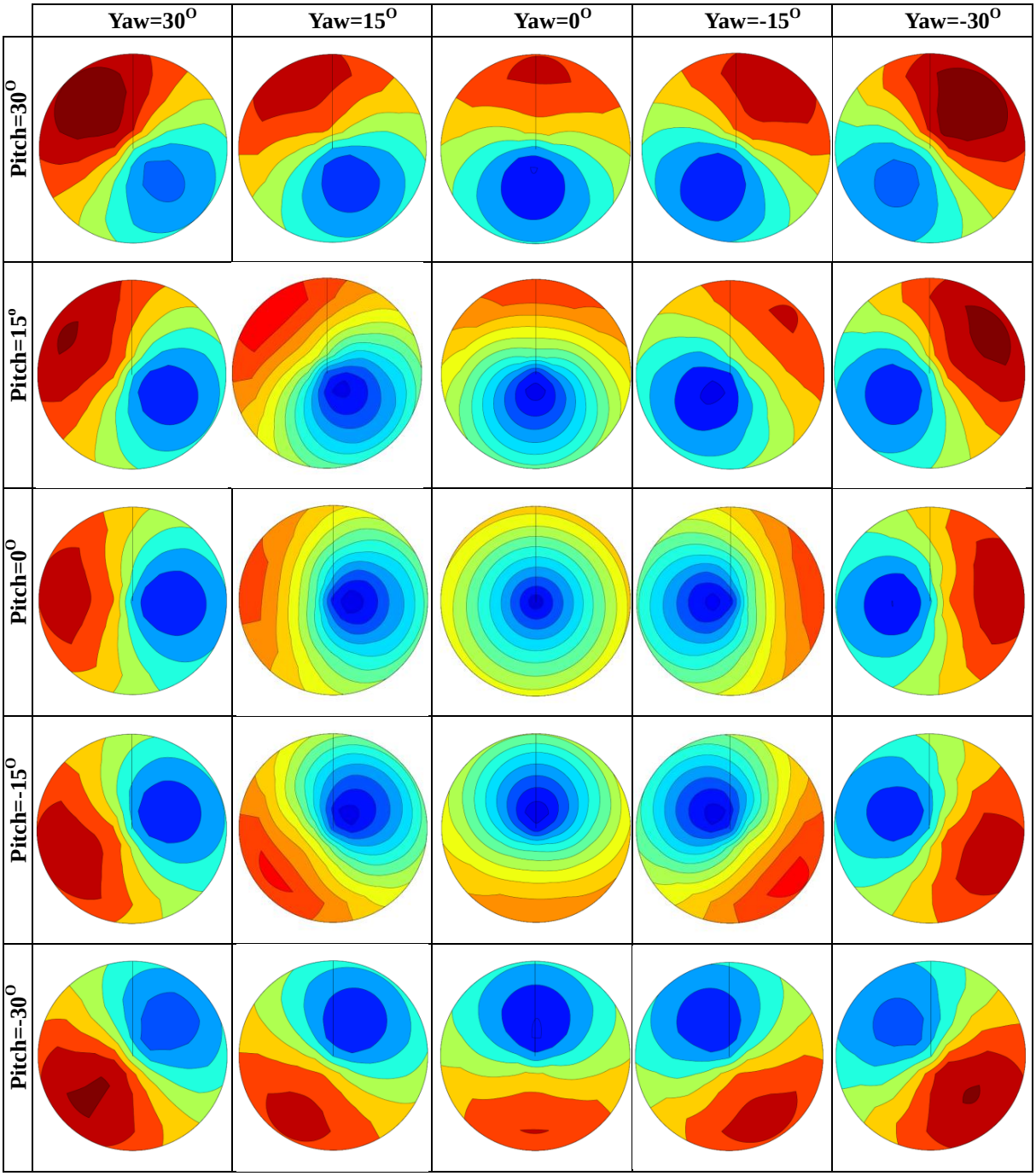

Fig. 10 : Pressure contours on the nose cone's surface

Except for the taping that belongs to the largest diameter p6 all the other tapings pressure measurements have very little differences between them. Each of the pressure lines in Fig.12 is unique for the particular yaw and pitch angle combination and its shape depends also on the flows total and static pressure and consequently on the flows velocity. The last observation clarifies that there is a non linear functional dependence between the pressure readings of each sensor and the flows velocity, as expected from the energy equation. This means that if a measurement takes place for the same yaw and pitch angle but for a different flow velocity, the pressure measurements will vary significantly. This issue has always been overcome by non-dimensionalisation methods as shown in the previous section for the two pressure sensor probe by estimating the velocity of the flow. That method requires at least two pressure tapings, even for the rotating pressure probe. In the methods presented in this section, only one pressure sensor is necessary.

In order to identify the most appropriate way to build the best calibration model, four variations of the model have been set up and tested with respect to their effectiveness.

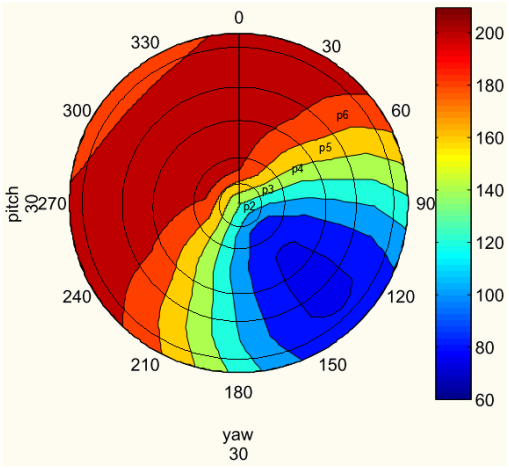

Fig. 11: Pressure contours on the nose cones surface and pressure tapings diameters

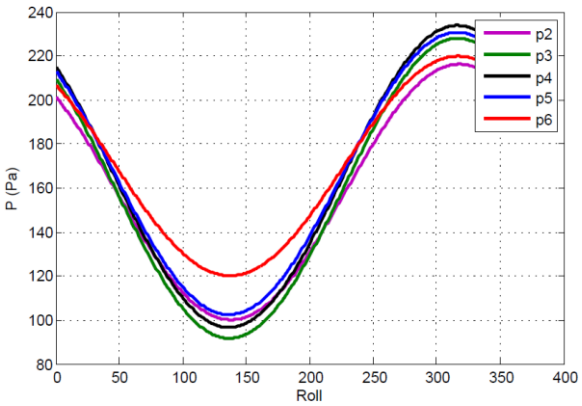

Fig. 12: Pressure readings of pressure tapings mounted on each one of the five selected diameters

1st model

The first model uses the sum of two pressure measurements with angular distance equal to 180^O. In the equations presented, the pressure measurements in 0^O and in 180^O are used, but the coefficients behaviour would be the same if the ones in 90^O and 270^O were to be used, instead.

$$Cp(i)pitch = \frac{P_i(180^0) - P_i(0^0)}{P_i(180^0) + P_i(0^0)} \quad (5)$$

$$Cp(i)yaw = \frac{P_i(90^0) - P_i(270^0)}{P_i(180^0) + P_i(0^0)} \quad (6)$$

$$Cp(i)static = \frac{P_i(180^0) + P_i(0^0) - \mathrm{Pst}}{P_i(180^0) + P_i(0^0)} \quad (7)$$

$$C(i)total = \frac{P_i(180^0) + P_i(0^0) - P_{\mathrm{tot}}}{P_i(180^0) + P_i(0^0)} \quad (8)$$

2nd model

The second model uses the maximum pressure estimated by the four pressure measurements, which occur at 0^O, 90^O, 180^O and 270^O. For example, in the case of the angular combination presented in Fig. 12 the pressure sensor mounted on the fourth diameter would give an estimation of the maximum pressure on that diameter, equal to 95 Pa approximately and the equivalent on the second diameter would give an estimation of 100 Pa.

$$Cp(i)pitch = \frac{P_i(180^0) - P_i(0^0)}{P_{max}} \quad (9)$$

$$Cp(i)yaw = \frac{P_i(90^0) - P_i(270^0)}{P_{max}} \quad (10)$$

$$Cp(i)static = \frac{P_{\max} - \mathrm{P}_{st}}{P_{max}} \quad (11)$$

$$Cp(i)total = \frac{\mathrm{Po} - P_{\max}}{P_{max}} \quad (12)$$

In Fig. 13 and Fig.14 the above calibration coefficients results can be observed. In the first figure, the CpPitch and CpStatic coefficients for the 1st model are presented and in the second the same coefficients for the 2nd model that makes use of the maximum pressure estimation. The mounting locations examined, are the first three diameters, as the corresponding results have been found to provide sufficient information for a full view on changes invoked by the sensors mounting position. Figs. 13 and 14 present diagrams on the same scale, in order to facilitate direct comparison. Also, the diagrams presented in Fig. 5 can be compared with them, too, despite the fact that they are plotted on different scale. The behaviour of the pitch coefficient is identical to the yaw coefficient, so the same conclusions can be drawn from both angle coefficients.

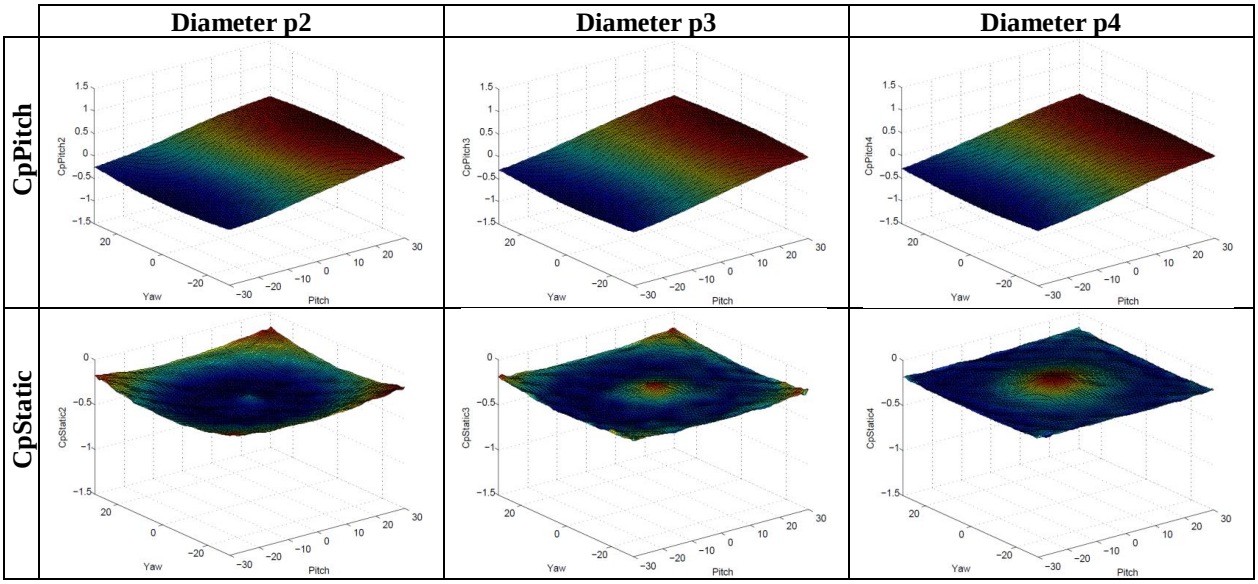

Fig. 13: Single pressure sensor calibration coefficients -CpPitch, CpStatic- model with the 1st model

Firstly, the sensitivity of these models differs, where the highest sensitivity belongs to the two sensor model presented earlier in this paper. Right next to that is the single sensor model with the maximum pressure estimation and the last is the single sensor model with no estimations. Secondly, regarding the coefficient variations according to the sensors mounting diameter, the single sensor models do not seem to have significant variations, whereas the variations of the two sensor model presented in the previous section were very intense with their sensitivity increasing as the diameter grows smaller. An important outcome of this observation is that the choice of the mounting place of the pressure transducer for those single pressure sensor models does not affect the coefficients behaviour. Hence, this choice can be made based on alternative criteria, such as the accommodation of the probes construction process. Thirdly, the reliability range for both last models presented is maximized since the coefficients behaviour, especially, for the first one is very smooth. This characteristic shows reliable results especially in comparison to the two pressure sensor model presented earlier, specifically for the smaller diameters. So according to the above analysis the maximum pressure estimating calibration method is the most efficient since it has the highest sensitivity.

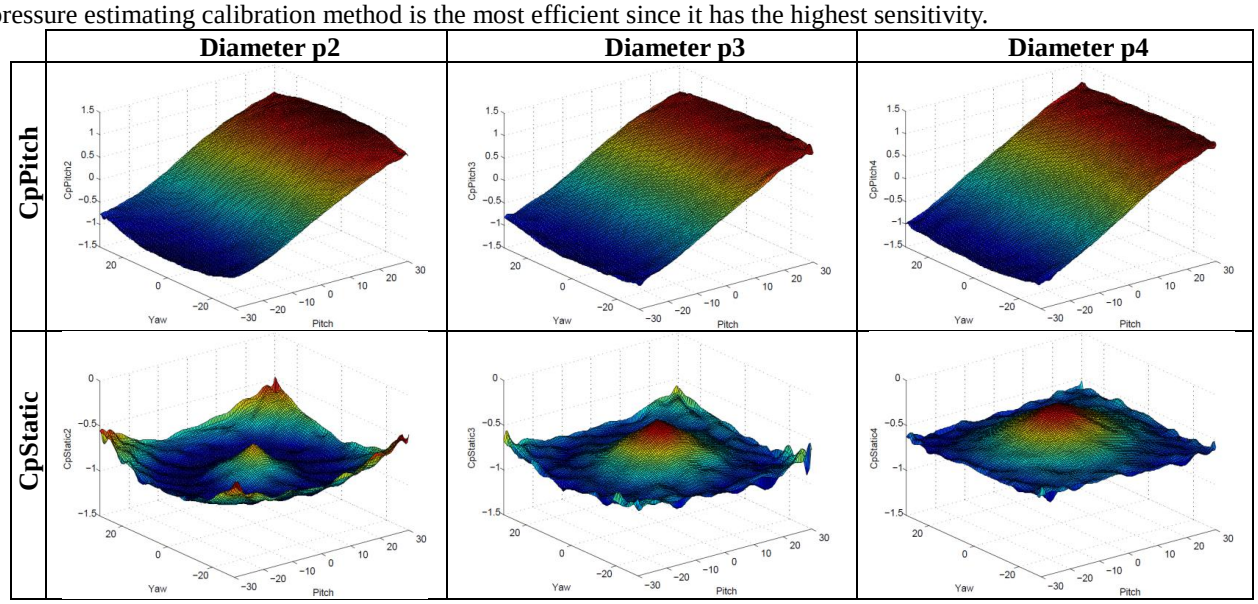

Fig. 14: Single pressure sensor calibration coefficients -CpPitch, CpStatic- model with the 2nd model

3rd model

In this model the yaw and pitch coefficients are the same with the ones presented in 2nd model, but for the determination of the total and static pressure the following coefficients are used (eq.13 and 14).

$$Cp(i)static = \frac{P_{st} - P_1}{P_{max} - P_{min}} \tag{13}$$

$$Cp(i)total = \frac{\mathrm{P}_1 - P_{\mathrm{tot}}}{\mathrm{P}_{\max} - P_{min}} \quad (14)$$

Where, P_1 is the pressure on the tip of the nose cone while the P_{max} and P_{min} are the maximum and minimum pressures over the whole surface of the cone, for each particular combination of yaw and pitch angles, respectively. The static and total pressure coefficients behaviour is presented in Fig. 15 and 16.

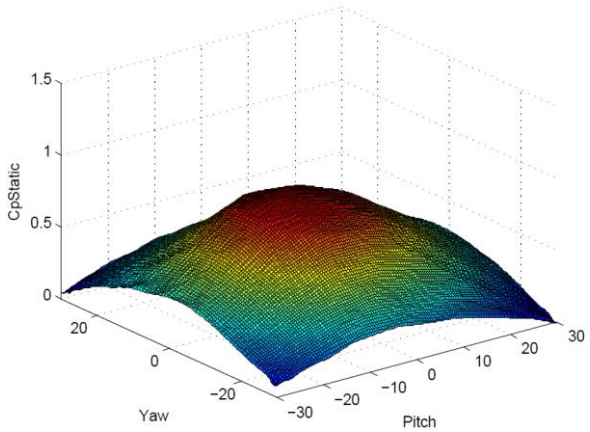

Fig. 15: Static pressure coefficient (eq. 13)

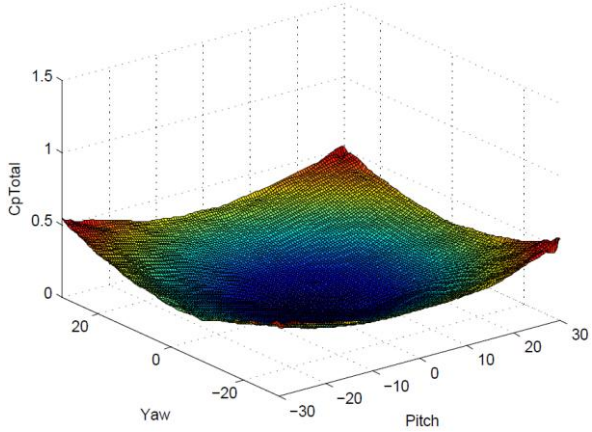

Fig. 16 : Total pressure coefficient (eq. 14)

This calibration method requires the non-dimensionalization of the surfaces pressure contours with a specific pressure that belongs to a certain diameter. So, if the pressure sensor chosen belongs to, e.g., the diameter p4, for each angular combination, the maximum pressure of this diameter is used for the division of all pressures on the surface. Thus a new index similar to the one presented in Fig. 10 is formed. In this case, the maximum pressure occurring on the diameter p4 for each particular angular combination is used to divide each pressure on the surface.

4th model

This method is based on the diagram of Fig. 12 and the fact that each pressure sensor after a full rotation gives a unique combination of pressure measurements for a predefined combination of yaw and pitch angles. Hence, the calibration method is very similar to the 3rd model. The difference is that no angular coefficients are used. In their place, for each angular combination all five different pressure sensors measurements for a full rotation are saved. Then a certain sensor is chosen, e.g., the one belonging to p4 whose maximum pressure measured in each angular combination after a full rotation is used for the non-dimensionalisation of all the pressure measurements occurred in this angular combination, as in the previous model. This sensor is essentially the one that will be used in the actual measuring process. The total and static pressures are estimated using the same coefficients and methodology as with the 3rd model.

MEASURING METHODOLOGY WITH THE PRESENTED CALIBRATION MODELS

In all cases, the measuring process is similar to a three or a five hole-probe, except for the necessity for the probe's rotation. Each calibration method has its own measuring methodology, by which all the necessary characteristics of the flow are obtained. As in every measuring process, the absolute barometric pressure has to be determined by a barometer in order to calculate the exact total pressure of the flow.

For each specific measurement there must be a certain sample of measurements the average of which is extracted. The sample should be at least larger than 5 so that uncertainties will be minimized. The stability of the flow as well as the accuracy of the measuring equipment is critical for the sampling range required.

In the case of using those models with a wind turbine nose cone, the determination of the angular position can be made firstly by noticing mechanically a specific angle as the 0^O angle. Then, the amount of time required for covering a single degree is known by automatically dividing the amount of time required for a full rotation by 360^O. So, every actual angular position can be determined.

Two pressure sensor probe, 1st model

Firstly the probe enters a flow according to the calibration axes and obtains a measurement. Then it bears a 90^O rotation and the second measurement takes place. This partial rotation is repeated three times in order to obtain all the necessary measurements for the calibration coefficients.

When all the necessary measurements are obtained, the yaw and pitch angles can be determined. Through them the total and static pressure can be extracted from their calibration diagrams. Hence, the flows velocity can be determined.

The appropriate mounting diameter for the second transducer may be chosen according to the goal. If high sensitivity is required for a small angular range, the diameter should be small. On the other hand, if larger angular range combined with larger reliability is required, a larger diameter should be chosen.

Single pressure sensor probe, 1st model

This model is very similar to the previous one. It only differs in the use of a single pressure sensor instead of two. Firstly, the angular coefficients are determined, which combined with the calibration diagrams provide the flow angles. Then, total and static pressures are determined through the total and the static coefficients. The nose cone's tip sensor is disabled. The mounting of the sensor can be anywhere between the five diameters presented in Fig.2 since, as shown in the diagrams of Fig.13, there is no particular variation in them.

Single pressure sensor probe, 2nd model

For the single pressure probe with the maximum pressure estimation, an extra step will be necessary in order to complete the measuring process. This step requires the estimation of the maximum pressure, by a certain mathematical model, such as a Fourier polynomial. The sensor may be taken as if it would obtain measurements continuously for a whole rotation. The remaining procedure is the same as for the previous models.

Single pressure sensor probe, 3rd model

In this model the angular coefficients used are the same with the last model. After the determination of the flow's angles, the index that contains the nondimensionalised pressures of the whole cones surface can be obtained through the calibration process. Thus if that index gets multiplied with the maximum pressure estimated from the sensor that belongs to the chosen pressure tapping diameter e.g. p4, the actual pressures on the whole cone's surface will come up as result. After that, the maximum and minimum pressure on the surface are acquainted as well as the pressure on the cones tip, which by now can determine through eq.13 and eq.14 the total and static pressure of the flow and hence its velocity. Since in this model no matter which mounting diameter is chosen, the static and total pressures coefficients are the same, the only difference is in the angular ones, which as mentioned before have no significant influences by changes in the sensors mounting place.

Single pressure sensor probe, 4th model

The basic difference between this model and all the others is that the measurements to be taken do not have to be in specific angular positions, except for the first one and also they don't have to be of a certain number. According to the Nyquist theorem for the determination of every periodical signal only two values of it are necessary. In this case it is best if at least three values are obtained after a full rotation with the first one to be made in a known angular position, which should be the 0^O.

The next two or more measurements can take place in any other angular position in the same rotation. This flexibility in the measuring positions makes this model the most easy to handle and also the most easy to accomplish, since no angular position recognition mechanism in every 90^O is necessary, except for the recognition of the 0^O angular position.

Hence, a simple way to make sure that all the measurements take place in the same rotation is to compute the time required for a full rotation and then to take all the required measurements in a smaller amount of time.

Having obtained the required measurements, the pressure combinations of the chosen sensor are estimated e.g. the sensor in the p4 diameter and a specific curve is produced, similar to the ones presented in Fig. 12, by which the maximum pressure can be estimated.

All pressures are divided by the maximum pressure, in order to produce the previous curve in a nondimensionalised form. All possible combinations of angles have been saved nondimensionalised and so a pattern recognition can be developed, by which the pitch and yaw angles can be defined. Finally, the total and static pressure of the flow can be defined by eq. 13 and eq. 14 as presented earlier.

WING BLOCKAGE EFFECT ON THE CALLIBRATION COEFFICIENTS

The until now the presented models and measurements, refer to a wind turbines nose cone without its wings mounted, as it is shown in Fig.4. In order to investigate their possible effects on the pressure combinations that the cones surface bears, three simulation wings were constructed and mounted on it.

Then the same measurements took place for the diameter p4, so that a comparison between them could be made. In Fig. 17 and Fig 18 can be seen that the two angular coefficients are strongly affected by the existence of the wings. This means that for the use of this cone as a dynamically measuring pressure probe, the calibration coefficients have to be recalculated.

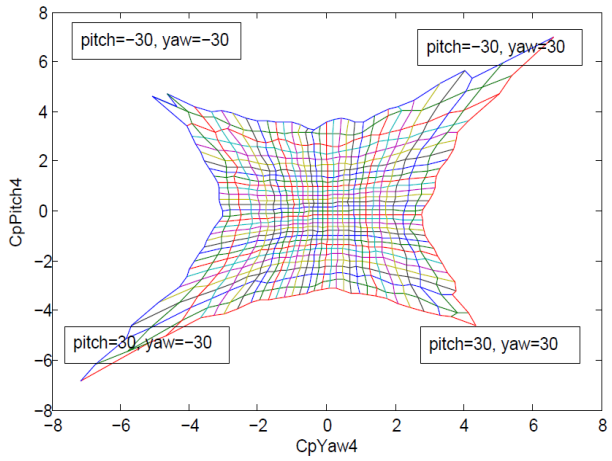

Fig. 17 : CpPitch-CpYaw coefficients for p4 diameter without wings

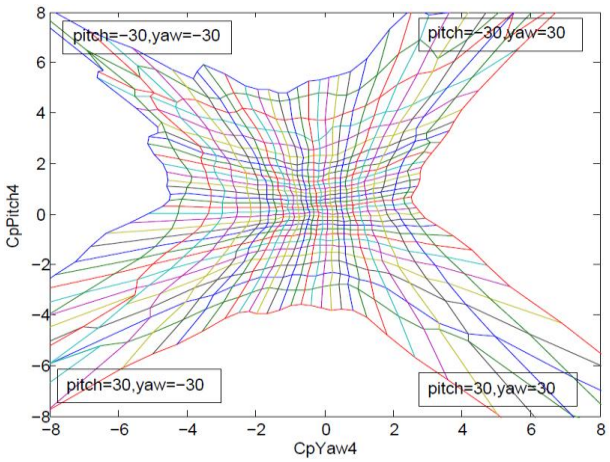

Fig. 8 : CpPitch-CpYaw coefficients for p4 diameter with wings

INVESTIGATION OF THE NONDIMENSIONALISATION QUANTITIES

In the previous pages, five different calibration models were presented for the same pressure probe with four different sets of calibration coefficients. Regardless of the fact that each set of coefficients had a different behaviour, all of them had parts that were the same. In this section, the basic parts (numerator-denominator) of those coefficients will be analysed separately in order to obtain conclusions about the influences of each one in each coefficient's result.

Coefficients numerator

Each coefficient presented has a numerator whose role is to react in any changes occurring in the variable that this coefficient is responsible for.

$$P_i(180^0) - P_i(0^0) \tag{15}$$

$$P_i(90^0) - P_i(270^0) \tag{16}$$

No matter which calibration model is used the numerators of the angular coefficients are the same differential quantities that maximize the sensitivity in any angular changes of the flows vector presented by the quantities of eq.15 and eq.16 and can be seen in Fig.19.

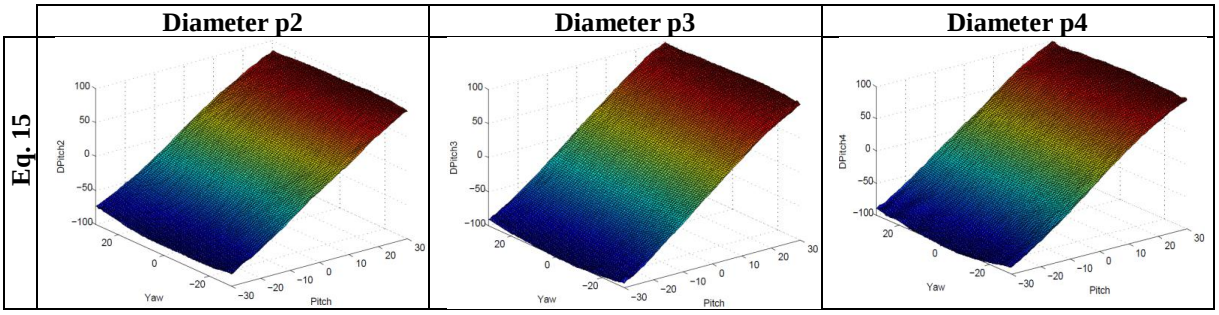

Fig. 19: Equation 15 results for three different diameters

The 17 to 22 quantities represent the numerator of static and total pressure coefficients respectively and in Fig. 20 and Fig. 21 the behaviour of the first two is presented. The basic difference and at the same time drawback of them comparing to the angular ones is the fact that they are not differential. This happens because in a certain flow the total and static pressures are dimensionless constants.

$$P_1 - \mathrm{Pst} \tag{17}$$

$$\mathrm{Po} - P_1 \tag{18}$$

$$P_i(180^0) + P_i(0^0) - \mathrm{Pst} \tag{19}$$

$$P_i(180^0) + P_i(0^0) - P_{\mathrm{tot}} \tag{20}$$

$$P_{\max} - \mathrm{Pst} \tag{21}$$

$$\mathrm{Po} - P_{\max} \tag{22}$$

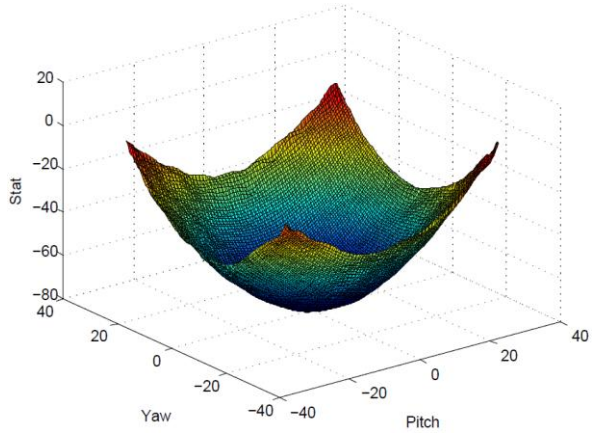

Fig. 20: Equation 17 results

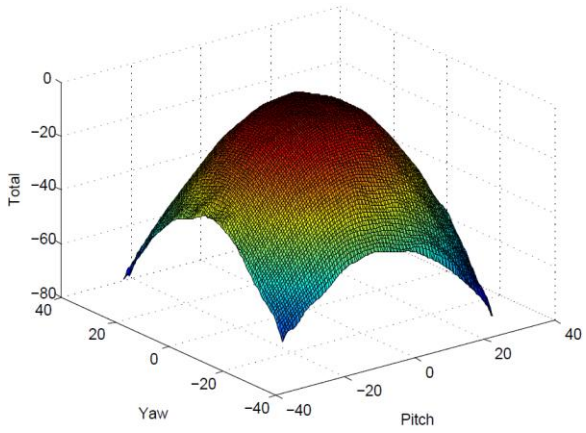

Fig. 21: Equation 18 results

Coefficients denominator

The ability to use each coefficient in flows with different static and total pressure from the flow used for the calibration of the probe depends on nondimensionalisation process. This process takes place by adding a denominator to the quantity that calculates the situation of the flows characteristic it has been charged with.

Bellow four different nondimensionalisation quantities are presented where eq. 23 belongs to the two sensor model while eq. 24 to 27 belong to the single sensor model. The results of eq. 24 and eq.25 are actually the same, since they measure pressures with angular distance equal to 180^{O}.

$$P_1 - (P_i(0^0) + P_i(90^0) + P_i(180^0) + P_i(270^0))/4 \quad (23)$$

$$P_i(180^0) + P_i(0^0) \quad (24)$$

$$P_i(90^0) + P_i(270^0) \quad (25)$$

$$P_{\max} \quad (26)$$

$$P_{max} - P_{min} \quad (27)$$

In Fig.22 the behaviour of the non-dimensionalisation quantities is presented providing a complete survey of the impact of each one on the coefficient it is used in. The first conclusion that can easily be conducted is that each quantity has a different scale. Hence, the smallest one belongs to eq.23 which belongs to the two sensor probe and follows the eq. 26 for the single pressure probe with the maximum pressure estimation. The largest scale belongs to eq. 24, which corresponds to the single pressure probe without estimations.

Observation and comparison of Fig. 5, Fig. 13 and Fig. 14 show that the smaller the scale of the non-dimensionalisation quantity, the larger is the sensitivity of the coefficient according to changes in the flows characteristic it is charged with. Thus, the two sensor probe has the largest sensitivity, and the single sensor pressure probe follows, with the least sensitivity belonging to the model without the estimation of the maximum pressure.

The second characteristic of the coefficients besides their sensitivity is their reliability, a characteristic that concerning the two sensor calibration model was shown to decrease as the coefficients sensitivity increased. The same behaviour can be noticed in Fig. 22 for eq. 23, which obviously is responsible for the two sensor model coefficients behaviour, since their numerator is very smooth for all the diameters.

Although the denominators of the other two models, have in some cases a very smooth behaviour, this cannot be seen in the counterpart of their coefficients. This is, also, because of the scale of the denominators, which in this case are much smaller compared to the two sensor calibration method. e.g. for the two sensor case an alteration from 5 Pa to 10 Pa is a 100% change which strongly determines the coefficients result. On the other hand for the single sensor case an alteration from 330 Pa to 340 Pa is an about 3% alteration which does not have much of an influence in the smoothness of the coefficients diagram.

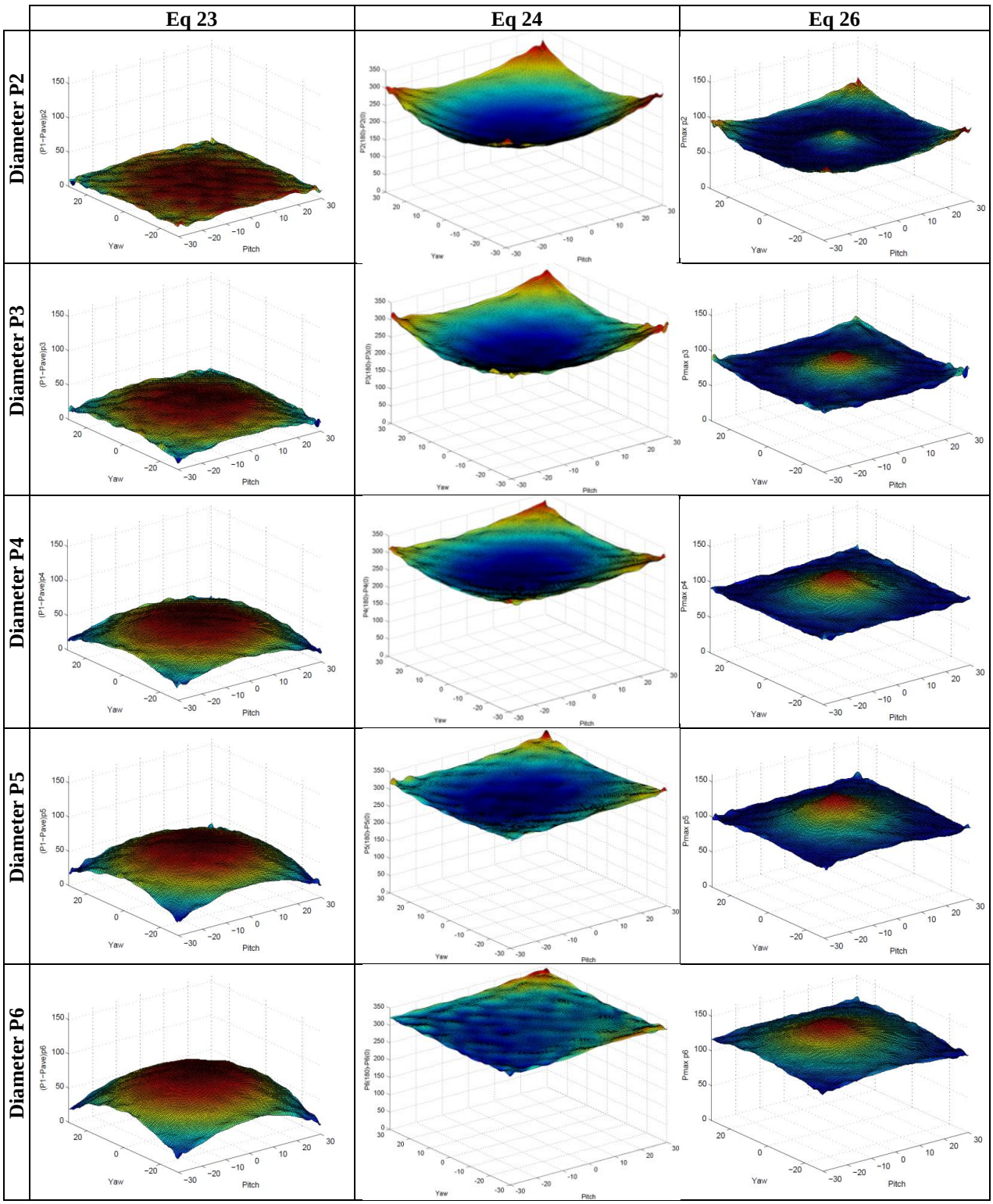

Fig. 22 : Coefficients denominator dependency on yaw and pitch angles

Therefore, in order to achieve the same range of sensitivity in flow changes between the two sensor model and the single sensor model, there will be necessary a much more sensitive-accurate pressure meter as well as more stable flow. Finally, Fig. 23 presents the quantity of eq. 27, which is used as a denominator in the total and static pressure coefficients of the 3rd and 4th calibration models.

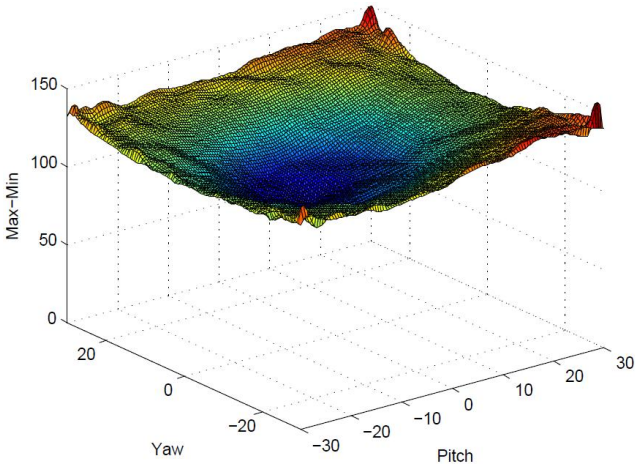

Fig. 23 : Coefficients denominator Eq 27

CONCLUSIONS

A small wind turbines cone was aerodynamically examined and successfully calibrated as a rotating single pressure probe which has the ability to define all the characteristics of a 3D flow by four distinctive single pressure probe calibration methods. In order to compare those models with a commonly used five-hole probe a rotating two pressure sensor calibration model was implemented for the same cone.

The two pressure sensors coefficients behaviour depended strongly on the peripheral sensors mounting diameter, leading to growth of their sensitivity and diminishing of their reliability as expected. On the contrary as concerns the single sensor models, the mounting diameter of the measuring sensor induced such small changes to the coefficients that they could be neglected. The above facts depend on the innovative normalization quantities that were used for each single sensor model, which were separately examined from the coefficients for further understanding. From the models used the best was the one that made use of the maximum pressure estimation during a whole rotation of the probe. Furthermore, the alterations that the blockage effect of the blades causes to the calibration coefficients were investigated proving that they are considerable.

The presented calibration models are appropriate for use not only by any wind turbine nose cone but with any pressure probe that has the ability to rotate and has axial symmetry. This leads to revolutionary calibration models that have similar capabilities with a common five-hole probe but require smaller and easier to construct probes with simplified calibration methods and most important of all a single pressure sensor mounted anywhere on the probes surface. Those characteristics result to a cost reduction in a 3D flow measurement equal to at least the manufacturing cost difference between the two mentioned probes.

REFERENCES

[1] J. Schlienger, A. Pfau, A.I. Kalfas, R.S. Abhari (2002) ‘’Single pressure transducer probe for 3d flow measurements’’ 16th Symposium on Measuring Techniques in Transonic and Supersonic Flow in Cascades and Turbomachines Cambridge, UK September 2002.

[2] Tanaka, K, Kalfas, AI, and Hodson, HP (2000), Development of Single Sensor Fast Response Pressure Probes, XVth Symposium on Measuring Techniques in Transonic and Supersonic Flows in Cascades and Turbomachines, Florence, Italy.

[3] Babinsky H., Kuschel U., Hodson H. P., Moore D. F. Welland M. E. (2000) ‘’ The Aerodynamic Design and Use of Multi-Sensor Pressure Probes for MEMS Applications’’ XV Symposium on measuring techniques in turbomachinery Sep 21-22 Firenze Italy.

[4] Antivachis K.N., (2011) ‘’Wind flows vector determination through a single pressure sensor mounted on a wind turbines nose cone’’ Diploma thesis, Dep. of Mechanical Engineering Aristotle University of Thessaloniki.

[5] Gossweiler C. (1993) On Probes and Measuring Techniques for Fast-Response Flow Measurement Using Piezo-Resistive Pressure Transducers, Dissertation ETH No. 10253, ETH Zurich, Switzerland

[6] Gossweiler C. (1996) Unsteady Measurements with Fast Response Probes, Von Karman Institute for Fluid Dynamics, Bruxelles, Lecture series 1996-01.

[7] Kupferschmied P., Gossweiler C. (1992), Calibration, Modelling and Data Evaluation Procedures for Aerodynamic Multihole Pressure Probes on the Example of a Four Hole Probe, Proc. 11th Symp. on Meas. Tech. for Transonic and Supersonic Flows in Cascades and Turbomachines, Munich, Germany.

[8] Barigozzi G., Dossena V., Gaetani P., Development and First Application of a Single Hole Fast Response Pressure Probe, 15th Symposium on Measuring Techniques for Transonic and Supersonic Flows in Cascades andTurbomachines, Florence, Italy, Sep 28-29.